NMR study of Aliquat and C8mim based magnetic and non-magnetic ionic liquids

Rui Cordeiro (nº72846)

We performed ^{1}H longitudinal NMR relaxometry and diffusometry study of mixtures of 1 %(v/v) of [Aliquat][FeCl4] with [Aliquat][Cl] and DMSO in different concentrations: 50 %(v/v) DMSO-d6, 50 %(v/v) DMSO-h6 and 99 %(v/v) DMSO-h6, respectively. Experimental data obtained in [18] for samples with 0 %,1% and 10 % (v/v) DMSO-d6 was refitted to a single exponential and is also presented. In order to isolate the paramagnetic relaxation from other relaxation mechanisms, the same techniques were used to analyse similar samples without [Aliquat][FeCl4]. X-ray diffraction profiles were also collected for all samples.

The results obtained show that the paramagnetic relaxation enhancement (PRE) present in $[Aliquat]^+$ based ferromagnetic ionic liquids attenuates for high DMSO concentrations. The decrease on the PRE seems to be caused by the fact that DMSO solvates $[FeCl_4]^-$ ions.

We also performed similar studies in $[C_8mim]^+$ based magnetic ionic liquids, discovering that this system also exhibits PRE. The PRE measured is less intense than in $[Aliquat]^+$ systems, mainly due to a faster diffusion of $[FeCl_4]^-$ ions in this system when compared to $[Aliquat]^+$.

I. INTRODUCTION

The term "Ionic liquid" describes a wide class of liquids which are composed entirely by ions. Room temperature ionic liquids (RTIL) are those which have melting point below 100 ºC, and as a class were discovered around one hundred years ago, being the first one of the RTIL, ethylammonium nitrate, synthesised in 1914 by Paul Walden [1]. RTIL are generally comprised by organic cations and inorganic anions, and have a wide set of interesting properties [2, 3], such as a wide liquid range, negligible vapor pressure, high thermal stability, non-flammability and good intrinsic conductivity. These properties make ionic liquids very interesting for future applications and a hot topic of research. Possible applications include chemical separation [4], electrodeposition of aluminum [5], gas storage [6], its use in lithium ion batteries [7], cellulose dissolution [8] and as a catalyst in chemical processes [9, 10]. However, none looks more promising than the role as solvents, since its very low vapor pressure means they almost do not evaporate. This means less atmospheric contamination and associated health problems, but also an economic advantage as solvent is not wasted. This and the fact that they are usually non-flammable earned them the label of "green solvents" [11]. Most importantly, the fact that both the cation and the anion can be changed allows the handler to modify the properties of the liquid to its necessities. The number of possible combinations is believed to be in the vicinity of 10^6 for binary ionic liquids, an number which quickly rises if tertiary ionic liquids are considered [12], which basically entails an endless source of combinations to probe for specific applications. This amazing tuneability is at the heart of its promise as future green "designer solvents".

Magnetic ionic liquids (MIL) are ionic liquids that incorporate a paramagnetic component in either the cation or the anion. Most common MIL incorporate a transition metal or a lanthanide complex in its anion [13]. Magnetic ionic liquids have all the aforementioned properties of ionic liquids and are also affected by magnetic fields. Some properties, such as viscosity and diffusion coefficient also become magnetic field dependent. In the case of supported magnetic ionic liquid membranes, its permeability has also been found to depend on the magnetic field [14]. Recently, it has been suggested that MIL can also be used as contrast agents [15].

Recent studies [16] discovered significant paramagnetic relaxation enhancement (PRE) on $[Aliquat]^+$ based ferromagnetic ionic liquids. Subsequent studies [17, 18] analysed the effects of adding small quantities of a co-solvent (dimethyl sulfoxide - DMSO) to the ionic liquid mixture. These studies showed that replacing some of the $[Aliquat]^+$ for DMSO did not attenuate the PRE as might have been expected.

This work tries to build on those previous ones by extending the range of concentrations of the co-solvent in order to understand the underlying molecular dynamics responsible for the PRE in this kind of system. For that reason, we analysed mixtures of $[Aliquat]^+$ with increasing DMSO concentrations, namely 50%(v/v) and 99% (v/v). Furthermore, since the use of deuterated DMSO for the 99% mixture yields very small signals and is thus impractical, two different samples, one with deuterated and another with protonated DMSO were studied for the 50% (v/v) case in order to understand the effect of the DMSO protons' relaxation and to connect it to the 99% (v/v) case.

Since the paramagnetic relaxation was described by this work by two different models instead of the one model used for both [16–18], the same experimental data for the pure $[Aliquat]^+$ and 1% (v/v) and 10% (v/v) DMSO mixtures shown in [18] was refitted after being gently given by its authors. All this data for the different samples was then analysed and fitted together to give the full picture of the effect of gradually adding a co-solvent on the PRE for $[Aliquat]^+$ MIL/IL mixtures. Finally, in order to try to understand how much cation choice impacts the existence of the PRE, another cation, $[C_8mim]^+$, was used to prepare a $[C_8mim]^+$ based ferromagnetic ionic liquid which was then analysed.

Figures 1 and 2 display the two cations used in this

work, $[\text{Aliquat}]^+$ and $[\text{C}_8\text{mim}]^+$:

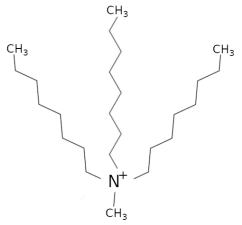

Figure 1. $[\text{Aliquat}]^+$ cation.

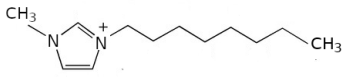

Figure 2. $[\text{C}_8\text{mim}]^+$ cation.

II. NUCLEAR MAGNETIC RESONANCE

Elementary particles possess a form of intrinsic angular momentum called spin. Nuclei are a collection of elementary particles, neutrons and protons, each with spin equal to $\frac{1}{2}$. The nuclei behaves as a single particle, with total spin angular momentum I. Choosing a direction (usually the direction of an external magnetic field), the projection of spin in that direction is given by the secondary spin quantum number m. There is a magnetic dipole moment $\hat{\mu} = \gamma\hbar\hat{I}$ associated with the spin of the nuclei, where γ is the gyromagnetic ratio, and its projection on the chosen direction is given by $\mu_z = \gamma\hbar m$. An isolated spin of magnetic moment $\hat{\mu}$ under a magnetic field $\vec{B} = \vec{B}_0$ has a Zeeman Hamiltonian:

$$\hat{\mathcal{H}}_Z = -\hat{\mu}.\vec{B}_0 = -\gamma\hbar\hat{I}.\vec{B}_0. \tag{1}$$

Its eigenvalues are the Zeeman levels:

$$E = -m\gamma\hbar B_0. \tag{2}$$

The first phase of any NMR experience is to generate a net magnetization on the substance to be studied, which means that only non zero spin nuclei can be observed using this techniques. For a given magnetic field $\vec{B} = B\hat{e}_z$ a net magnetization will appear in the same direction (the magnetic moments μ_y and μ_x average to 0, therefore there will be no magnetization on those axis), with amplitude given by:

$$\begin{aligned} M =& M_z = n\langle\mu_z\rangle = n\frac{\sum_{\mu_z=-\gamma\hbar I}^{\gamma\hbar I}\mu_z\ exp(-E_\mu/kT)}{\sum_{\mu_z=-\gamma\hbar I}^{\gamma\hbar I} exp(-E_\mu/kT)} \\ =& n\gamma\hbar\frac{\sum_{m=-I}^{I} m\ exp\left(\frac{\gamma\hbar mB}{kT}\right)}{\sum_{m=-I}^{I} exp\left(\frac{\gamma\hbar mB}{kT}\right)} \quad \left(x=\frac{\gamma\hbar BI}{kT}\right) \\ =& n\gamma\hbar I\frac{d}{dx}\left(ln\Big(\sum_{m=-I}^{I} exp\big(\frac{x}{I}m\big)\Big)\right) = n\gamma\hbar I B_I(x), \end{aligned} \tag{3}$$

where we used the Zeeman Hamiltonean ($E_\mu = -\mu_z B$) and the last function is called the Brillouin function, $B_I(x) = \frac{2I+1}{2I}coth(x + \frac{x}{2I}) - \frac{1}{2I}coth(\frac{x}{2I})$. For a proton, $x \approx 10^{-3}\frac{B}{T}$, which means that, as $\frac{B}{T}$ is at most of the order of 10^{-2}, $x \leq 10^{-5}$. This means that a high temperature/ low field approximation can be used. Expanding the Brillouin function in a Taylor series around $x = 0$ and keeping only the first term, we get:

$$M \approx \frac{1}{3}n\gamma\hbar(I+1)x = \frac{n\gamma^2\hbar^2 I(I+1)}{3kT}B = \frac{C}{T}B, \tag{4}$$

which is called the Curie law, with Curie constant $C = \frac{n\gamma^2\hbar^2 I(I+1)}{3k}$.

The interaction of the total magnetization with the applied magnetic field is described by a set of phenomenological equations called the Bloch equations. Just like an individual magnetic moment experiences a torque caused by a magnetic field, the same is true for the total magnetic moment per unit volume, i.e. the magnetization:

$$\frac{d\vec{M}}{dt} = \gamma\vec{M} \times \vec{B} \tag{5}$$

If the magnetization is not aligned with the magnetic field, it will experience a precession motion known as Larmor precession. The frequency is known as the Larmor frequency and is given by:

$$\omega_0 = -\gamma B_0, \tag{6}$$

in which the minus sign accounts for the direction of rotation. For instance, a proton has a positive gyromagnetic ratio and will therefore precess clockwise.

In order to perform an NMR experiment, this equilibrium magnetization needs to be perturbed. This is achieved by applying a radiofrequency field in resonance with the Larmor frequency of nucleus, which will displace the magnetization towards the x-y plane, which is called a pulse (of length t).

Thermal agitation constantly generates random magnetic fields at the nuclei. When the magnetization is displaced from its equilibrium value, these random magnetic fields will have a finite contribution at the frequencies that can induce transitions between spin polarization states,which means there is a finite probability of transition between these states, which will eventually put the spin system in thermal equilibrium with the lattice, with the equilibrium Boltzmann populations and the magnetization on the z-axis.

The return to the equilibrium is given by two times, T_1 and T_2. T_1 is the relaxation time for the z-component of the magnetization and is called longitudinal or *spin-lattice relaxation.* T_2 is the relaxation time for the x and y components of the magnetization and is called transverse or *spin-spin relaxation.* As the processes responsible for T_1 and T_2 aren't always the same (although every T_1 inducing process contributes to T_2), these times are

different. These relaxation constants can be added to the Bloch equations as following:

$$\frac{dM_x}{dt} = \gamma M_y B_z - \gamma M_z B_y - \frac{M_x}{T_2} \tag{7}$$

$$\frac{dM_y}{dt} = \gamma M_z B_x - \gamma M_x B_z - \frac{M_y}{T_2} \tag{8}$$

$$\frac{dM_z}{dt} = \gamma M_x B_y - \gamma M_y B_x - \frac{M_z - M_0}{T_1} \tag{9}$$

The study performed on this work revolves mainly on the measurement of the spin-lattice relaxation time T_1. As previously discussed, fluctuating magnetic fields at specific frequencies give rise to relaxation. Fluctuating magnetic fields can be generated by different kinds of movements, which constitute separate relaxation mechanisms. Different kinds of movements have specific correlation times associated to them, and the relaxation rate generated by them will be a function of this correlation time:

$$R_1 = \frac{1}{T_1} = E_c^2 f(\tau_n), \tag{10}$$

where E_c is the strenght of the interaction and τ_n the correlation time for the mechanism.

In most cases there will be a combination of more than one of these individual mechanisms. In such a case, it is usually assumed that they are independent, which implies that the total relaxation rate is simply the sum of the individual relaxation rates:

$$\frac{1}{T_1} = \sum_{n=1}^{N} \frac{1}{T_{1n}}, \tag{11}$$

where each n represents a relaxation mechanism ($n = 1$ for the rotational relaxation rate, $n = 2$ for the diffusion rate and so on for all relevant mechanisms). In the following sections a review of the mechanisms used in this work is provided:

A. Rotational diffusion

In the case of spins belonging to the same molecule, the distance between them is almost a constant and only the orientation of the vector between two spins changes in a significant way. This kind of intra-molecular relaxation corresponds to the relative rotational motion between magnetic dipoles and is therefore aptly called rotational diffusion.

In its famous paper [19], Bloembergen, Purcell and Pound (BPP) determined the spectral densities by assuming the rotation of a molecule as the rotation of a rigid sphere in a viscous medium. Using a diffusion equation for the angle between spins, they were able to calculate the following spectral densities:

$$J^{(0)}(\omega) = 6J^{(1)}(\omega) \tag{12}$$

$$J^{(1)}(\omega) = \frac{4}{15r^6}\frac{\tau_r}{1+\omega^2\tau_r^2} \tag{13}$$

$$J^{(2)}(\omega) = 4J^{(1)}(\omega), \tag{14}$$

in which r is the average distance between spins.

These densities allowed them to determine the relaxation time T_1. Using $I = \frac{1}{2}$ for both spins:

$$\left(\frac{1}{T_1}\right)_{Rot} = \frac{3}{10}\left(\frac{\mu_0}{4\pi}\right)^2 \frac{\gamma^4\hbar^2}{r^6}\left[\frac{\tau_r}{1+\omega^2\tau_r^2} + \frac{4\tau_r}{1+\omega^2\tau_r^2}\right], \tag{15}$$

which is the rotational rate used for this work.

B. Translational diffusion

In the case of two spins belonging to different molecules, both their respective distances and relative orientation are a function of time. The molecules to which they belong will diffuse with respect to one another, and therefore the relaxation caused by these movements is called translational diffusion.

A satisfactory result was derived by Torrey [20], which assumed that the molecules were trapped in a potential well, only allowed to move through a fast random jump between trapped states. He obtained the following spectral densities:

$$\begin{aligned} J^{(k)}(\omega,\tau_d) =& (4k^2-9k+6)\frac{8\pi n\langle r^2\rangle}{45d^5}\frac{1}{\omega^2\tau_d}[(u_+\left(1+\frac{1}{u_-^2+u_+^2}\right) \\ &+2)e^{-2u_+}\cos 2u_- + u_+\left(1-\frac{1}{u_-^2+u_+^2}\right) \\ &+u_-\left(1-\frac{1}{u_-^2+u_+^2}\right)e^{-2u_+}\sin 2u_-] \end{aligned} \tag{16}$$

with $u_\pm$ given by:

$$u_\pm = \frac{1}{2}\sqrt{\frac{q(1\pm q)}{\alpha}}, \tag{17}$$

and q equal to:

$$q = \frac{\omega\tau_d}{\sqrt{4+(\omega\tau_d)^2}}. \tag{18}$$

In the spectral densities, τ_d is the correlation time, $\langle r^2\rangle$ is the mean square jump distance, n is the spin density and d is the minimum distance of approach between the spins. The diffusion constant D enters the equation for the relaxation rate through the equality:

$$\langle r^2\rangle = 6\tau_d D. \tag{19}$$

C. Cross-relaxation

Nuclear spins with $I > \frac{1}{2}$ have an additional pathway for relaxation, namely electronic quadrupolar relaxation. If these spins are present in a given sample, there will be an effect of cross-relaxation to consider. Since there are chlorine nuclei in the samples to be studied, and both naturally ocurring isotopes ^{35}Cl and ^{37}Cl have spin $I = \frac{3}{2}$, it becomes necessary to include this effect. The relaxation rate has the following equation [21]:

$$\left(\frac{1}{T_1}\right)_{CR_n} = A_{CR_n}\frac{\tau_{CR_n}}{1+(\omega-\omega_{CR_n})^2\tau_{CR_n}^2}, \tag{20}$$

with A_{CR_n} being the strength of the interaction and τ_{CR_n} the correlation time associated with the various ω_{CR_n} frequencies. These frequencies are:

$$\omega_{CR_n} = \omega_Q \pm \gamma_{Cl}B_0\cos\phi, \tag{21}$$

with ω_Q given by:

$$\omega_Q = \frac{3e^2qQ}{4\hbar}, \tag{22}$$

where e is the charge of the electron, ϕ is the angle between the z axis of the electric field gradient tensor in the principal axis system of the chlorine nucleus and the external magnetic field and Q is the quadrupole moment.

D. Order parameter fluctuation

The liquids studied in this work are in the isotropic phase, and therefore show no preferred order as given by a director axis. However, there may be local order in small domains of the sample, caracterized by a local director and a local order parameter tensor.

This local order is not permanent, however, and relaxes with caracteristic time given by:

$$\tau_{OPF} = \frac{\xi^2\nu}{L}, \tag{23}$$

with ν being a phenomenological viscosity coefficient, ξ the lenght of the ordered domain and L an elastic constant.

The spectral density due to the order parameter fluctuations can be calculated [22]:

$$J_1(\omega) = \frac{k_BT\sqrt{\nu}}{4\sqrt{2}\pi L^{3/2}}\Big(\frac{\tau_0}{1+\sqrt{1+\omega^2\tau_{OPF}^2}}\Big)^{1/2}. \tag{24}$$

The formula used to fit the experimental data in this work is:

$$\frac{1}{T_1}_{OPF} = \frac{A_{opf}}{\sqrt{f}}\int_0^{f_{max}/f}\frac{\sqrt{x}}{1+(x+f_{min}/f)^2}dx, \tag{25}$$

in which f_{min} and f_{max} are respectively the minimum and maximum cutoff frequencies for the order parameter fluctuation (OPF) relaxation and $A_{opf} \propto \frac{\nu^{1/2}}{L^{3/2}}$. The maximum cutoff is directly related to the minimum distance involved in this fluctuation, which is the length of a single molecule, while the minimum cutoff relates to the maximum distance involved in the OPF, which is the size of the ordered domain.

E. Paramagnetic Relaxation

The presence of paramagnetic molecules in a sample is a very strong source for relaxation. Unpaired electrons' spin interacts with the nuclei spin and the modulation of this interaction will give rise to fast relaxation, being most often the dominant relaxation mechanism even for small quantities of the paramagnetic material.

The paramagnetic relaxation rate is a sum of different contributions. In this work, we will consider two different components, inner-sphere (IS) and outer-sphere (OS) relaxation:

$$\left(\frac{1}{T_1}\right)_p = \left(\frac{1}{T_1}\right)_{OS} + \left(\frac{1}{T_1}\right)_{IS} \tag{26}$$

1. Inner Sphere

The inner sphere contribution is due to the temporary coordination between protons and the paramagnetic particle. The relaxation due to this coordination is governed by two times, the relaxation time if the coordination is permanent and the mean lifetime of this coordination (the inverse of the exchange rate). Therefore, $\left(\frac{1}{T_1}\right)_{IS}$ is given by:

$$\left(\frac{1}{T_1}\right)_{IS} = \frac{P_m}{T_{1m}+\tau_m}, \tag{27}$$

where P_m is the mole fraction of bound solvent protons and τ_m is the mean lifetime of the coordination.

In the case of diluted solutions, which is valid for all samples studied in this work, P_m is given by:

$$P_m = qF\frac{m_s[m]'}{1000\rho}, \tag{28}$$

in which q is the number of solvent molecules connected to a paramagnetic particle, F is the fraction of protons of the molecule bound to the paramagnetic center, m_s is the molar mass of the solvent, ρ is the density of the solution in kg/L and $[m]'$ is the molar concentration of paramagnetic particles in $mmol/L$.

The relaxation rate in the absence of exchange is the sum of two components, one due to the dipole-dipole interaction between the unpaired electron and the proton

spin $\left(\frac{1}{T_{1m}^{dd}}\right)$ and one due to the contact interaction between them $\left(\frac{1}{T_{1m}^{sc}}\right)$, which are given by the following expressions [23]:

$$\frac{1}{T_{1m}^{dd}} = \frac{2}{15}\left(\frac{\mu_0}{4\pi}\right)^2 \frac{\gamma_S^2\gamma_I^2\hbar^2}{r_{IS}^6} S(S+1)\left[\frac{3\tau_{c1}}{1+\omega_I^2\tau_{c1}^2} + \frac{7\tau_{c2}}{1+\omega_S^2\tau_{c2}^2}\right] \tag{29}$$

$$\frac{1}{T_{1m}^{sc}} = \frac{2}{3}\left(\frac{A}{\hbar}\right)^2 S(S+1)\left[\frac{\tau_{e1}}{1+\omega_S^2\tau_{e1}^2}\right], \tag{30}$$

where γ_S is the gyromagnetic ratio of the electron and γ_I is the gyromagnetic ratio of the proton, r_{IS} is the distance between spins I and S and $A/\hbar$ is the Fermi-contact coupling constant between both spins.

The correlation times in both expressions are themselves a sum of different contributions:

$$\begin{aligned} \tau_{c1}^{-1} &= \tau_R^{-1} + T_{1e}^{-1} + \tau_m^{-1}, \\ \tau_{e1}^{-1} &= T_{1e}^{-1} + \tau_m^{-1}, \end{aligned} \tag{31}$$

in which τ_R is the rotational correlation time of the pair formed by the paramagnetic complex and the coordinated protons and T_{1e} is the electron longitudinal relaxation time. For $S > 1/2$, T_{1e} is given by the modulation of the zero field splitting interaction (ZFS) [24]. Although monoexponential analytical results are only valid for $S = 1$, for $S > 1$ the following result is valid in the case of extreme narrowing ($\omega_S\tau_v << 1$):

$$T_{1e}^{-1} = \frac{1}{25}\Delta^2[4S(S+1)-3]\left[\frac{\tau_v}{1+\omega_S^2\tau_v^2} + \frac{4\tau_v}{1+4\omega_S^2\tau_v^2}\right], \tag{32}$$

in which Δ is the average value of the ZFS interaction in units of s^{-1} and τ_v is the correlation time of the ZFS fluctuations.

2. Outer Sphere

The outer sphere contribution is the contribution generated by the diffusion of protons in the vicinity of paramagnetic centers. This contribution is given by [25]:

$$\begin{aligned} \frac{1}{T_{1\,OS}} =& \frac{32\pi}{405}\left(\frac{\mu_0}{4\pi}\right)^2 \gamma_S^2\gamma_I^2\hbar^2 \frac{n_m N_a}{aD} S(S+1) \\ & \times \left[j_2(\omega_I - \omega_S) + 3j_1(\omega_I) + 6j_2(\omega_I + \omega_S)\right], \end{aligned} \tag{33}$$

with ω_I and ω_S the proton and electron Larmor frequencies, n_m the spin density of the paramagnetic molecules and N_a the Avogadro number, a is the effective distance between the electron and proton spins and D is the effective diffusion coefficient given by the sum of the diffusion coefficients of both species ($D = D_I + D_S$).

The spectral densities j_k are given by:

$$j_k(\omega) = \frac{9}{4} Re\left\{\frac{4+z_k}{9+9z_k+4z_k^2+z_k^3}\right\}, \tag{34}$$

with

$$z_k = \sqrt{i\omega\tau_D + \tau_D/T_{ke}}, \tag{35}$$

where the diffusion correlation time τ_D satisfies $\tau_D = a^2/D$.

III. EXPERIMENTAL METHODS

The samples used in this work were prepared at the Faculdade de Ciências e Tecnologia - UNL and at the Faculdade de Farmácia - UL using a procedure described in references [26, 27]. The experimental techniques used in this work were NMR relaxometry, NMR diffusometry and X-ray diffractometry. NMR relaxometry forms the experimental core of this work, since all the models used to predict the microscopic dynamics of the system are made to fit the relaxometry curves obtained from this method. NMR diffusometry was used for measuring the diffusion constants of the samples, and X-ray diffractometry was used to extract information about the typical distances at the molecular level. Diffusion measurements were conducted at the CENIMAT at FCT/UNL using a 300MHz superconducting magnet with a *Bruker Diff 30* diffusion probe using a technique known as pulsed field gradient NMR (PFG). X-ray diffractometry measurements were made using the X-ray diffractometer in use at the Soft Matter Laboratory at IST. For the NMR relaxometry measurements, three different magnets were used, a desktop low field spectrometer [28] that can measure T_1 for proton Larmor frequencies ranging from 10 KHz to 9 MHz, a medium field iron core electromagnet capable of probing fields from 9 MHz to 90.5 MHz and a superconducting magnet that operates at 300 MHz.

IV. RESULTS AND DISCUSSION

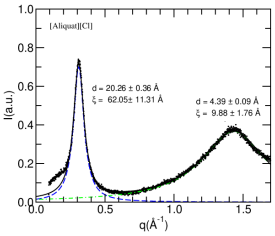

Figure 3. [Aliquat][Cl] X-ray diffractogram.

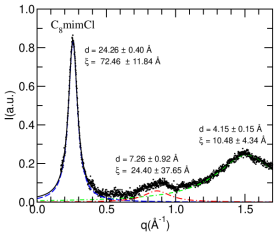

Figure 4. [C$_8$mim][Cl] X-ray diffractogram.

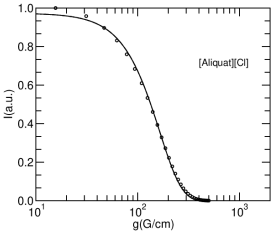

Figure 5. [Aliquat][Cl] diffusometry curve.

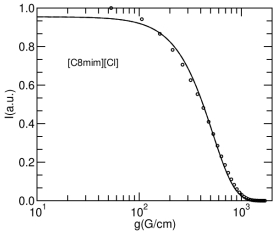

Figure 6. [C$_8$mim][Cl] diffusometry curve.

X-ray and diffusion measurements were made for all systems studied in this work, and figures 3, 4, 5 and 6 show X-ray diffraction spectra and diffusometry curves obtained for [C$_8$mim][Cl] and [Aliquat][Cl] .

X-ray measurements were used to determine distances at the molecular level, which were then used to fix distance parameters in the NMRD fitting process, namely the average jumping distance in the diffusion model, which was obtained by the peak representing the smaller distances, and the outer-sphere distance parameter, which was correlated to the peak representing the longest distances by assuming an effective outer-sphere distance of one fourth of that value.

The diffusion measurements were used to obtain the diffusion coefficients for the cation in the different samples.

A. DMSO effect on [Aliquat]$^+$ based IL and MIL

In order to understand the effect of DMSO in the PRE displayed by [Aliquat]$^+$ based MIL, [Aliquat][Cl] samples with 1%(v/v) [Aliquat][FeCl$_4$] and various DMSO concentrations were studied. These DMSO concentrations were respectively 0,1%,10%,50% and 99%(v/v) DMSO (deuterated DMSO for all except 99%). Since the 99% DMSO sample used DMSO-h6 to display a strong enough signal, a second 50% (v/v) DMSO-h6 sample was also studied, to understand the effect of the DMSO protons' relaxation on the NMRD. Since there are several relaxation mechanisms acting together with paramagnetic relaxation, samples of [Aliquat][Cl] with the same DMSO concentration but without 1%(v/v) [Aliquat][FeCl$_4$] were also studied. These samples were used to determine all the relaxation mechanisms' parameters except for the ones of the paramagnetic relaxation, while the samples with 1%(v/v) [Aliquat][FeCl$_4$] were used exclusively to determine the paramagnetic relaxation.

Figure 13 shows the nuclear magnetic relaxation dispersion (NMRD) data and fitting curves for all samples without [Aliquat][FeCl$_4$] , ordered by increasing DMSO concentration.

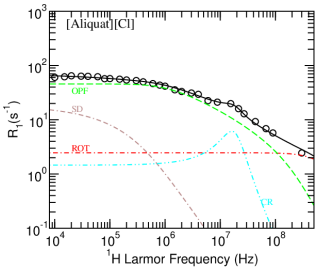

Figure 7. 0% DMSO

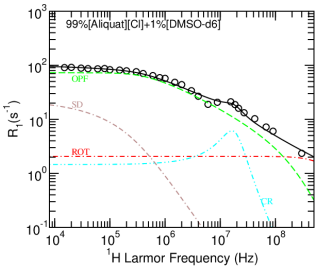

Figure 8. 1% DMSO-d6(v/v)

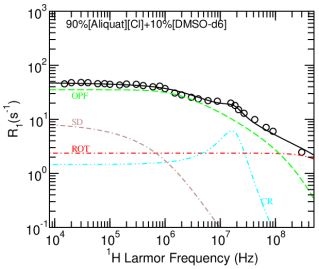

Figure 9. 10% DMSO-d6(v/v)

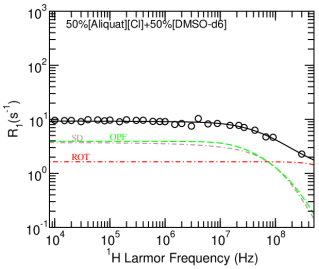

Figure 10. 50% DMSO-d6(v/v)

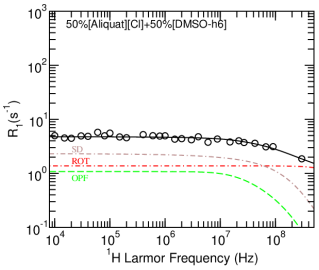

Figure 11. 50% DMSO-h6(v/v)

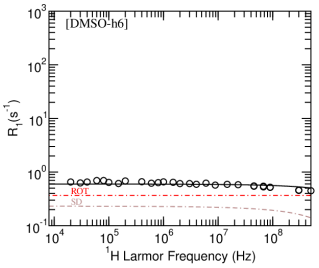

Figure 12. 99% DMSO-h6(v/v)

Figure 13. All [Aliquat]$^+$ based non-paramagnetic samples' NMRD (ordered by DMSO percentage).

Of the mechanisms common to all samples, the rotational mechanism has the smallest relaxation contribution, as seen in 13. The samples with 0,1 and 10% (v/v) DMSO-d6 had similar correlation times, implying similar average rotation speeds for the [Aliquat]$^+$ molecules in these samples. For bigger concentrations of DMSO, a noticeable decrease in rotational correlation times was found. Since smaller correlation times imply faster rotation, the smaller correlation time for 50% (v/v) DMSO-d6 compared to the samples with less DMSO is evidence

for a faster average rotation of $[Aliquat]^+$ molecules with increasing DMSO concentration. There is also a decrease in correlation times from the deuterated to the protonated 50% (v/v) DMSO samples, due to the faster rotation of DMSO compared to $[Aliquat]^+$.

For the diffusion mechanism, there is an enormous difference between the distance of lateral closest approach from 0,1 and 10 % (v/v) DMSO-d6 samples and the other, which seems to be consistent with fundamentally different kinds of diffusion. For the 0,1 and 10% (v/v) DMSO-d6 the distances obtained are consistent with the distances between the center of mass of two contiguous $[Aliquat]^+$ molecules, which suggests that the diffusion is made by the molecule as a whole, and that there is no liberty of motion between the aliphatic chains. For the 50% (v/v) DMSO-d6 case, the distance obtained is consistent with the distance between aliphatic chains, suggesting the the diffusion we indirectly observe is the individual diffusion of each chain. This seems to imply that while small quantities of DMSO do not fundamentally alter the diffusion of $[Aliquat]^+$ molecules, bigger quantities of DMSO free up the individual chains, allowing them to diffuse independently of the main $[Aliquat]^+$ molecule.

Cross relaxation was a relatively weak mechanism, which was present at the 0, 1 and 10% (v/v) but not found for higher DMSO concentrations.

For the OPF mechanism, the minimum cutoff frequency increased with DMSO concentration, with the exception of the sample with 1%(v/v) DMSO. This increase of f_min implies a decrease in the maximum distance for the OPF mechanism with the addition of DMSO, which seems to indicate that the presence of DMSO, for moderate (10% (v/v)) to high (50% (v/v)) concentrations, gradually destroys the long range coordination of $[Aliquat]^+$ molecules. The exception of the 1% (v/v) DMSO case seems to indicate that DMSO, in lower concentrations, actually helps this long range coordination and increases the size of the correlated $[Aliquat]^+$ domains.

It is also important to mention that while analysing the experimental data, it was found that it was possible to make either the OPF mechanism or the diffusional mechanism dominant over the other. While initially it was reasoned that the diffusion curve should be the dominant one, new data for pure [Aliquat][Cl] samples at different temperatures ([29]) shows that a coherent analysis can only be performed if the OPF mechanism is the dominant one, since it was the only way to ensure that the f_{min} of the OPF mechanism did not decrease with temperature for the [Aliquat][Cl] samples, which would imply that the correlated domains would actually increase in size with temperature, a fact that seems implausible.

With all other mechanisms discussed, it is now time to analyse all samples with 1%(v/v) $[Aliquat][FeCl_4]$. Figure 13 shows the nuclear magnetic relaxation dispersion (NMRD) data and fitting curves for all samples without $[Aliquat][FeCl_4]$, ordered by increasing DMSO concentration. All other contributions apart from paramagnetic relaxation were summed into a single "Bulk" curve.

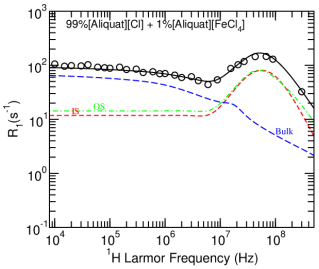

Figure 14. 0% DMSO

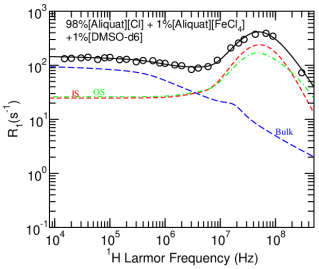

Figure 15. 1% DMSO-d6 (v/v)

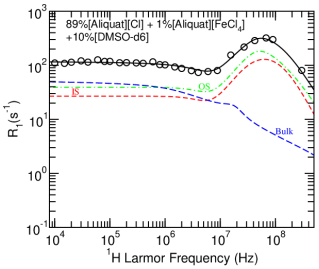

Figure 16. 10% DMSO-d6 (v/v)

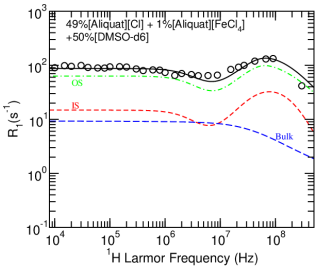

Figure 17. 50% DMSO-d6 (v/v)

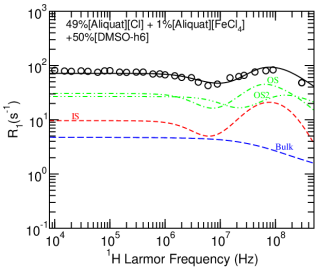

Figure 18. 50% DMSO-h6 (v/v)

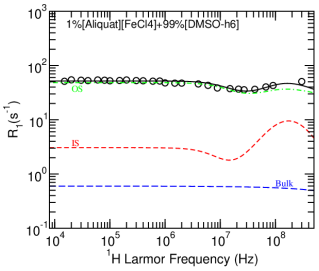

Figure 19. 99% DMSO-h6 (v/v)

Figure 20. All $[Aliquat]^+$ based paramagnetic samples' NMRD (IS in red, both OS in green, Bulk in blue, ordered by DMSO percentage).

The value of Δ is a measure of the total energy of the ZFS interaction and is directly connected to the immediate vicinity of the $[FeCl_4]^-$ ion. It was reasonable to assume that since the $[FeCl_4]^-$ ions reside mainly in the polar areas of the $[Aliquat]^+$ molecules, the value of Δ should be reasonably independent of the quantity of DMSO and the numerical fitting of the data was made for a single value of Δ for every sample with deuterated DMSO. The fact that the sample with 99 % (v/v) DMSO-h6 had to be adjusted with a much higher value for Δ led us to make the assumption that this represents a fundamentally different chemical environment for the $[FeCl_4]^-$ ions in this sample, namely that it is mostly solvated by the DMSO molecules instead of residing in the polar areas of the $[Aliquat]^+$ molecules. The fact that the balance between IS and OS seems to be roughly 1:1

in the samples with 0%, 1 % and 10% (v/v) DMSO-d6 while the OS gains relative relevance for the 50% and 99% (v/v) DMSO-h6 samples seems to corroborate that there is solvation by DMSO for the 50% and 99% (v/v) DMSO samples.

For the 50% (v/v) DMSO-h6 case, since both $[Aliquat]^+$ and DMSO protons are now visible, one should observe $[FeCl_4]^-$ ions both solvated and in the polar areas of the $[Aliquat]^+$ molecules. This led to a numerical fit consisting in a weighted sum between two different OS, one with each Δ. The IS was assumed to have Δ corresponding to the non-solvated $[FeCl_4]^-$ ions. The weighted sum's factor was called the solvation factor $G = 0.34 \pm 0.05$, which seems to indicate that in the 50% (v/v) DMSO samples 34% of all proton relaxation by OS is due to solvated $[FeCl_4]^-$ ions. Knowing this solvation factor, it is possible to estimate the fraction of $[FeCl_4]^-$ ions that are solvated by DMSO molecules for the 50%(v/v) DMSO-h6 sample (which should be the same for the 50%(v/v) DMSO-d6 sample). It was found that this fraction is somewhere in the interval $[0.29; 0.47]$, meaning that the percentage of $[FeCl_4]^-$ ions solvated by DMSO molecules is at least 29% and at most 47%.

The rotational correlation time for the inner sphere mechanism, τ_{ISrot}, is a measure of the rotational speed of the complex formed by the $[Aliquat]^+$ molecule and the $[FeCl_4]^-$ ion. It decreases with DMSO concentration, which means that the rotation of the complex becomes faster with DMSO concentration. This means that while the addition of 1% (v/v) DMSO does not fundamentally alter the rotational dynamic of the $[Aliquat][FeCl_4]$ complex, larger concentrations do, starting from at least 10% (v/v) DMSO. They do so in a way such that the rotation becomes faster, which seems to imply that the presence of enough DMSO liberates the rotation of the complex.

The distance between spins for the IS mechanism, d_{in}, is an average of the distance between the $[FeCl_4]^-$ ion and the $[Aliquat]^+$ protons participating in the IS relaxation. The distance is relatively constant, excluding the sample without DMSO, which is higher. This seems to imply that the presence of DMSO, even in small quantities, approximates the $[FeCl_4]^-$ ion from the polar areas of the $[Aliquat]^+$ molecule, while increasing the DMSO quantity to higher concentrations seems to have no further effect.

There is a constant decrease in the distance between spins for the OS interaction. The values up to 50 % (v/v) DMSO describe the OS mechanism in the vicinity of the $[Aliquat]^+$ protons, and this decrease seems to suggest again that the presence of DMSO approximates the $[FeCl_4]^-$ ion from the $[Aliquat]^+$ molecule.

B. $[C_8mim]^+$ based samples

Figure 23 shows the NMRD data and fitting curves for $[C_8mim][Cl]$ and 99%(v/v)$[C_8mim][Cl]$ + 1%(v/v)$[C_8mim][FeCl_4]$.

There is no visible cross relaxation contribution on the $[C_8mim]^+$ sample, and therefore this mechanism was not used in the fitting.

For the rotational contribution, there is virtually no difference between rotational correlation times of $[C_8mim][Cl]$ and $[Aliquat][Cl]$, which seems to suggest that the rotational speeds of both cations are the same.

For the diffusion contribution, there are some fundamental differences between the two cations. The diffusion coefficient for $[C_8mim][Cl]$ is smaller than for $[Aliquat][Cl]$. Both average jump distances (r) are similar, while the distance of lateral closest approach (d) is very different. The big difference between the distance of lateral closest approach for both samples is explained by the fact that, for $[Aliquat]^+$, the diffusion is made by the molecule as a whole, and the distance is of the order of the distances between the center of mass of two contiguous $[Aliquat]^+$ molecules, while for $[C_8mim]^+$, a smaller molecule with only one aliphatic chain, this distance is simply of the order of the distance between molecules, which is also of the same order as r.

For the OPF contribution, there is a big difference between samples. While the intensity of the overall mechanism seems to increase for the $[C_8mim][Cl]$ sample, the minimum cutoff frequency increases by a factor of roughly ten, implying a much shorter distance for the domains of correlated $[C_8mim]^+$ molecules in comparison to the $[Aliquat]^+$ molecules. The maximum cutoff frequency decreases for the $[C_8mim][Cl]$ sample, which is surprising, since the $[C_8mim]^+$ molecule has a smaller size.

With the non-paramagnetic contributions already discussed, it is time to focus on the differences between paramagnetic relaxation when the cation is changed from $[Aliquat]^+$ to $[C_8mim]^+$.

The values of Δ are different for the different samples, which is most likely simply a consequence of the different chemical surroundings for the $[FeCl_4]^-$ ions.

The value of τ_v is bigger for the 99%(v/v)$[C_8mim][Cl]$ + 1%(v/v)$[C_8mim][FeCl_4]$ sample than its value for the 99%(v/v)$[Aliquat][Cl]$ + 1%(v/v)$[Aliquat][FeCl_4]$ sample. Since τ_v is modulated by collisions of the $[FeCl_4]^-$ ion with its surroundings, this appears to imply that

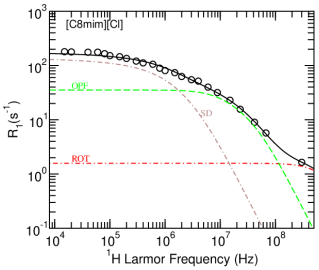

Figure 21. $[C_8mim][Cl]$

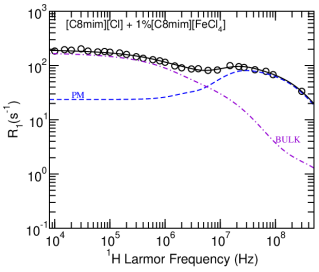

Figure 22. $[C_8mim][Cl]$ +1%(v/v)$[C_8mim][FeCl_4]$

Figure 23. $[C_8mim][Cl]$ and 99%(v/v)$[C_8mim][Cl]$ +1%(v/v)$[C_8mim][FeCl_4]$ NMRD.

there is a smaller frequency of collisions for the $[FeCl_4]^-$ ions when the cation is $[C_8mim]^+$ than when the cation is $[Aliquat]^+$.

Both diffusions, that of the cation (D_{MIL}) and of the anion (D_{an}) are bigger for the 99%(v/v)[C_8mim][Cl] +1%(v/v)[C_8mim][$FeCl_4$] sample than for the 99%(v/v)[Aliquat][Cl]+1%(v/v)[Aliquat][$FeCl_4$] sample. While the change of value for D_{MIL} does not alter the shape of the NMRD in a substantial way, the fourfold increase in the diffusion of the anion has a profound effect on it, severely decreasing the relaxation rate in the high frequency region, and therefore the PRE, for the sample with [C_8mim][$FeCl_4$] when compared to the sample with [Aliquat][$FeCl_4$] .

As for the rotational correlation time for the inner sphere mechanism, τ_{ISrot}, there is a twofold increase in its value for the sample with [C_8mim][$FeCl_4$] when compared to the sample with [Aliquat][$FeCl_4$] . This seems to indicate that the [C_8mim][$FeCl_4$] complex rotates slower than the [Aliquat][$FeCl_4$] complex does.

Both distances, the one associated with the IS mechanism (d_{in}) and the one associated with the OS mechanism (d_{out}) are bigger for the 99%(v/v)[C_8mim][Cl] +1%(v/v)[C_8mim][$FeCl_4$] sample than for the 99%(v/v)[Aliquat][Cl]+1%(v/v)[Aliquat][$FeCl_4$] sample. This is the second main factor (along with the bigger value for D_{an}) contributing for the reduction of the PRE in the sample with [C_8mim][$FeCl_4$] when compared to the sample with [Aliquat][$FeCl_4$] .

Finally, it is important to mention that the concentration of paramagnetic particles is bigger for the 99%(v/v)[C_8mim][Cl]+1%(v/v)[C_8mim][$FeCl_4$] sample than for the 99%(v/v)[Aliquat][Cl]+ 1%(v/v)[Aliquat][$FeCl_4$] sample. This makes the paramagnetic part of the NMRD of the sample with [C_8mim][$FeCl_4$] greater by a factor of $\frac{26}{12} \approx 2.17$ than it should be if we were to compare it in equal conditions to the 99%(v/v)[Aliquat][Cl] + 1%(v/v)[Aliquat][$FeCl_4$] NMRD curve. This makes the reduction of the PRE, already visible when comparing the NMRD curves, even more apparent.

V. CONCLUSIONS

One of the two main purposes of this work was to discover the effect on the PRE displayed by $[Aliquat]^+$ based ferromagnetic ionic liquids by the addition of a co-solvent, in this case DMSO. This goal has been fulfilled, and it has been observed that, while for relatively small quantities of DMSO (1 and 10% (v/v)) there was no notable attenuation of this PRE, for 50%(v/v) and 99% (v/v) there was a substantial reduction.

This reduction appears to be caused by the fact that the addition of large quantities of DMSO effectively separates some of the $[FeCl_4]^-$ ions from the $[Aliquat]^+$ cations, causing a reduction of the IS mechanism by disassembling some of the [Aliquat][$FeCl_4$] complexes.

The other main objective was to discover what happened to the PRE if the cation is changed. This comparison was made with another, simpler cation, $[C_8mim]^+$, and it showed that changing the cation dramatically alters the PRE. In this specific case, 99%(v/v)[C_8mim][Cl] + 1%(v/v)[C_8mim][$FeCl_4$] exhibits a lower relaxation rate due to paramagnetic relaxation mechanisms than 99%(v/v)[Aliquat][Cl] + 1%(v/v)[Aliquat][$FeCl_4$].

This difference seems to be mainly caused by a faster diffusion of the $[FeCl_4]^-$ ions in the sample with [C_8mim][$FeCl_4$] , suggesting that bigger PRE can be generated in systems where this diffusion is slowed.

Another important conclusion to retrieve from this work is the major importance of collective motions in the relaxation rate of both $[C_8mim]^+$ and $[Aliquat]^+$ based ionic liquid systems. These collective motions seem to be attenuated by the presence of larger quantities of DMSO, but exist at least up to 50%(v/v).

VI. FUTURE WORK

The results obtained in this work would benefit from an accurate determination of the diffusion coefficient for the $[FeCl_4]^-$ ions. It would also be useful to better understand the regions between 10% and 50%(v/v) DMSO and 50% and 99%(v/v) DMSO, by studying intermediate systems with DMSO concentrations between those studied in this work. Also, it would be important to study different cations with dimensions and structure between $[C_8mim]^+$ and $[Aliquat]^+$ cations, to see if the PRE is something between those obtained in this work or radically different. Furthermore, studying systems with other anions, such as $GdCl_6{}^{3-}$, would help to understand the effect of the metal anion used. Finally, it would be interesting to compare the results obtained in this work with molecular dynamics simulations [30].

ACKNOWLEDGMENTS

I would like to express my gratitude towards my supervisors, Pedro Sebastião and Carla Daniel, for their diligent support and advice throughout this study. I would also like to acknowledge my friend and colleague Maria Beira for all the support and exchange of ideas which greatly enriched this work.

[1] P. Walden. Molecular weights and electrical conductivity of several fused salts. Bulletin de l'Académie impériale des sciences de St. Pétersbourg,1914.

[2] K. Seddon. Ionic Liquids for Clean Technology. Journal of Chemical Technology & Biotechnology, **68**:351-356,1997.

[3] K. Marsh, J. Boxall, R. Lichtenthaler. Room temperature ionic liquids and their mixtures—a review. Fluid Phase Equilibria, **219**(1):93-98,2004.

[4] A. Berthod, M. Ruiz-Ángel, S. Carda-Broch.Ionic liquids in separation techniques. Journal of Chromatography A, **1184**(1):6-18,2008.

[5] T. Jiang, M. Brym, G. Dubé, A. Lasia, G. Brisard. Electrodeposition of aluminium from ionic liquids: Part I—electrodeposition and surface morphology of aluminium from aluminium chloride (AlCl3)–1-ethyl-3-methylimidazolium chloride ([EMIm]Cl) ionic liquids. Surface and Coatings Technology, **201**(1):1-9,2006.

[6] D. Tempel, P. Henderson, J. Brzozowski, R. Pearlstein, H. Cheng. High Gas Storage Capacities for Ionic Liquids through Chemical Complexation. Journal of the American Chemical Society, **130**(2):400-401,2008.

[7] M. Ishikawa, T. Sugimoto, M. Kikuta, E. Ishiko, M. Kono. Pure ionic liquid electrolytes compatible with a graphitized carbon negative electrode in rechargeable lithium-ion batteries. Journal of Power Sources, **162**(1):658 - 662,2006.

[8] R. Remsing, R. Swatloski, R. Rogers, G. Moyna. Mechanism of cellulose dissolution in the ionic liquid 1-n-butyl-3-methylimidazolium chloride: a 13C and 35/37Cl NMR relaxation study on model systems. Chemical Communications, **12**:1271-1273,2006.

[9] J. Sun, W. Cheng, W. Fan, Y. Wang, Z. Meng, S. Zhang. Reusable and efficient polymer-supported task-specific ionic liquid catalyst for cycloaddition of epoxide with CO2. Catalysis Today, **148**(3):361 - 367,2009.

[10] S. Ding, M. Radosz, Y. Shen. Ionic Liquid Catalyst for Biphasic Atom Transfer Radical Polymerization of Methyl Methacrylate. Macromolecules, **38**(14):5921-5928,2005.

[11] S. Mallakpour, M. Dinari. Green Solvents II. Springer, 2012.

[12] R. Rogers and K. Seddon. Ionic Liquids–Solvents of the Future? Science, **302**(5646):792–793,2003.

[13] E. Santos, J. Albo, A. Irabien. Magnetic ionic liquids: synthesis, properties and applications. RSC Advances, **4**(75):40008-40018,2014.

[14] E. Santos, J. Albo. C. Daniel, C. Portugal, J. Crespo, A. Irabien. Permeability modulation of Supported Magnetic Ionic Liquid Membranes (SMILMs) by an external magnetic field. Journal of Membrane Science, **430**:56-61,2013.

[15] C. Daniel, F. Chávez, C. Portugal, J. Crespo, P. Sebastião. ^{1}H NMR Relaxation Study of a Magnetic Ionic Liquid as a Potential Contrast Agent. The Journal of Physical Chemistry B, **119**(35):11740-11747,2015.

[16] Carla I. Daniel and Fabián Vaca Chávez and Gabriel Feio, Carla A.M. Portugal, João G. Crespo, Pedro J. Sebastião. ^{1}H NMR relaxometry, viscometry and PFG NMR studies of magnetic and nonmagnetic ionic liquids. The Journal of Physical Chemistry B, **117**(39):11877–11884,2013.

[17] M. Beira. NMR study of the molecular dynamics in magnetic and non-magnetic ionic liquids. Master thesis, Instituto Superior Técnico - Universidade de Lisboa, 2016.

[18] M. Beira, C. Daniel, P. Almeida, M. Corvo, A. Rosatella, C. Afonso, P. Sebastião. 1H NMR Relaxometry and Diffusometry Study of Magnetic and Nonmagnetic Ionic Liquid-Based Solutions: Cosolvent and Temperature Effects. The Journal of Physical Chemistry B, **121**(51):11472-11484,2017.

[19] N. Bloembergen, E. M. Purcell, R. V. Pound. Relaxation effect in nuclear magnetic resonance absorption. Physical Review, **73**(7):679–712,1948.

[20] H. C. Torrey. Nuclear Spin Relaxation by translational diffusion. Physical Review, **92**(4):962–969,1953.

[21] R. Kimmich, F. Winter, W. Nusser, K.H. Spohn. Interactions and fluctuations deduced from proton field – cycling relaxation spectroscopy of polypeptides, DNA, muscles, and algae. Journal of Magnetic Resonance, **68**:263–282,1986.

[22] R. Dong. Nuclear Magnetic Resonance of Liquid Crystals. Springer, 1997.

[23] N. Bloembergen, L. O. Morgan. Proton Relaxation Times in Paramagnetic Solutions. Effects of Electron Spin Relaxation.Journal of Chemical Physics, **34**(3):842-850,1961.

[24] A. Carrington, G.R. Luckhurst . Electron spin resonance line widths of transition metal ions in solution. Relaxation through zero-field splitting. Molecular Physics, **8**(2):125-132,1964.

[25] A. Merbach, L. Helm, E. Tóth. The Chemistry of Contrast Agents in Medical Magnetic Resonance Imaging. Wiley, 2013.

[26] R. Sesto, T. McCleskey, A. Burrell, G. Baker, J Thompson, B. Scott, J. Wilkes, P. Williams. Structure and magnetic behavior of transition metal based ionic liquids. Chemical communications, **28**(4):447-449,2008.

[27] J. Albo, E. Santos, L. Neves, S. Simeonov, C. Afonso, J. Crespo, A. Irabien. Separation performance of CO_2 through Supported Magnetic Ionic Liquid Membranes (SMILMs). Separation and Purification Technology, **97**:26-33,2012.

[28] D. Sousa, G. Marques, J. Cascais, P. Sebastião . Desktop fast-field cycling nuclear magnetic resonance relaxometer. Solid State Nuclear Magnetic Resonance, **38**(1):36-43,2010.

[29] AliquatCl NMRD for different temperatures - part of an article to be published - gently ceded by Maria Beira.

[30] P. Morgado, K. Shimizu, J. Esperança, P. Reis, L. Rebelo, J. Lopes, E. Filipe. Using 129Xe NMR to Probe the Structure of Ionic Liquids. The Journal of Physical Chemistry Letters, **4**(16):2758-2762,2013.